Comparison of different small-scale cultivation methods towards the valorization of a marine benthic diatom strain for lipid production

Mary Dianne Grace Arnaldo, Nadeeshani Dehel Gamage, Agathe Jaffrenou, Vony Rabesaotra, Aurélie Mossion, Gaëtane Wielgosz-Collin, Vona Méléder

PII: S2211-9264(23)00360-0

DOI: https://doi.org/10.1016/j.algal.2023.103327

Reference: ALGAL 103327

To appear in: *Algal Research*

Received date: 30 June 2023

Revised date: 13 November 2023

Accepted date: 14 November 2023

Please cite this article as: M.D.G. Arnaldo, N.D. Gamage, A. Jaffrenou, et al., Comparison of different small-scale cultivation methods towards the valorization of a marine benthic diatom strain for lipid production, *Algal Research* (2023), https://doi.org/10.1016/j.algal.2023.103327

Comparison of different small-scale cultivation methods towards the valorization of a marine benthic diatom strain for lipid production

Mary Dianne Grace Arnaldo, Nadeeshani Dehel Gamage, Agathe Jaffrenou, Vony Rabesaotra, Aurélie Mossion, Gaëtane Wielgosz-Collin, Vona Méléder*

*Corresponding author: Vona Méléder, vona.meleder@univ-nantes.fr

Nantes Université, Institut des Substances et Organismes de la Mer, ISOMer, UR 2160, F-44000 Nantes, France

Highlights

- A commercial suspension PBR was adapted to build a vertical tubular lab-scale PSBR
- Marine benthic diatom *Amphora* sp. NCC169 was cultivated in Fernbach flasks and PSBR
- Diatom biomass and lipid yield in PSBR are higher than in Fernbach flasks

Abstract

Marine benthic diatoms have the capacity to produce quality biomass and bioactive compounds for various commercial applications. *Amphora* sp. NCC169 is one of such species that have high-value lipid production. However, mass-production of *Amphora* sp. NCC169 in traditional suspension photobioreactor is challenged by its sensitivity to stirring and turbulence. The aim of this study is to compare the biomass and lipid productivity of *Amphora* sp. NCC169 cultures between a Fernbach flask and a low-maintenance, laboratory-scale culture system adapted from previously described vertically oriented porous substrate bioreactor (PSBR) designs. Results revealed that cells in the PSBR could achieve significantly higher biomass productivity ($P_{biomass}$ = 0.51 ± 0.05 g·m^{-2}·day^{-1}) and lipid productivity (P_{lipid} = 0.10 ± 0.03 g·m^{-2}·day^{-1}) than those in Fernbach flasks after 20 days of cultivation ($P_{biomass}$ = 0.29 ± 0.01 g m^{-2} day^{-1} ; P_{lipid} = 0.07 ± 0.01 g·m^{-2}·day^{-1}). Cellular photosynthetic efficiency

remained favorable in both culture conditions (F_v/F_m > 0.5) for the duration of the experiments.

Keywords: *Amphora* sp., immobilized photobioreactor, marine benthic diatoms, lipids

1. Introduction

Microalgae are promising candidates for biotechnological research, and they have become one of the major focus of development and innovation. Significant attention is gearing towards the study of diatoms, a major group of photosynthetic microalgae characterized by their silica cell walls. They dominate the primary production in coastal and estuarine environments, prevailing over 50% of some of the world's most productive marine food webs[1,2]. Considerable scientific interest is given to their outstanding physical properties and their corresponding potential in biotechnology.

Diatoms are reported to have competitive advantage over other species of similarly-sized microalgae under suitable controlled conditions, given the fact that they multiply rapidly, they have more advanced carbon flux metabolism, and almost 100% of their biomass can be utilized[3,4]. They are also highlighted for their ability to produce promising bioactive compounds with widespread industrial and pharmaceutical applications[5–8]. The importance of diatoms as primary producers is largely due to their high lipid content. Typical lipid fractions from diatoms were recorded to be at 15 to 25% of their dry weight, but some strains could reach lipid levels of up to 70 to 85% through regulation of the culture conditions[3,9,10]. They produce copious amounts of lipids as metabolites, with the neutral fraction accounting for almost 70% of the total lipids. Diatoms have high diversity of lipid composition, such as membrane-bound polar lipids, triglycerides, and lipid-derived free fatty acids[3]. They were shown to possess lipids such as eicosapentaenoic acid (EPA) and phytosterols that are promising for their nutritional value and bioactivity.

Traditionally, diatoms are produced using either of the two most common methods of microalgae cultivation: (a) open system such as carboys, tanks, and ponds, or (b) closed cultivation systems using photobioreactors (PBRs). The main difference between the two systems is linked to the cost, mode of

operation, and vulnerability to external factors[11,12].

Classical open cultivation systems account to approximately 95% of the total global microalgae production[13]. Open culture systems have relatively inexpensive construction and operation cost because they are almost always located outdoors and rely on natural light for illumination. They can also utilize runoffs and effluents to supply nutrients to microalgae[14]. On the other hand, they are susceptible to prevailing external conditions such as rainfall, temperature, and light intensity for the same reasons. Contaminants and predators like ciliates and rotifers can outcompete the cultured species and wreck the entire batch of operation.

Photobioreactors are increasingly being used for microalgae research and development because of their numerous advantages over open culture systems. Among the benefits include easier control of the culture parameters (e.g., temperature, pH), reduced contamination, higher productivity, and lower harvesting cost[15]. They are mainly used to grow axenic, monospecific cultures for the production of high-value compounds[16,17]. Several diatom species such as *Chaetoceros calcitrans*, *Skeletonema costatum,* and *Phaeodactylum tricornutum* have already been cultivated successfully in PBRs[18–20].

Cultivation of planktonic microalgal species predominate both open and closed cultivation systems. Hence, high resource/energy consumption and dewatering problems arise during harvesting, which is a major bottleneck for the biomass industry. Over the past two decades, biofilm cultivation systems present a novel strategy to circumvent these issues. In this system, microalgal cells that naturally have the capacity to bind to surfaces in their own exopolysaccharides (EPS) are provided with substrates to attach and proliferate. Majority of biofilm systems use solid non-porous substrates which uniquely serve as physical support for microalgal adhesion. This facilitates the application and diffusion of all relevant growth parameters (i.e. light, nutrients, gas exchange) on the same side of the substrate. These solid substrates can either be partially or completely submerged in the culture medium[21]. A porous substrate photobioreactor (PSBR), on contrary, is installed with a hydrophilic, microporous substrate which receives the culture media nutrients on one side while providing attachment and direct light and gas exchange to the biofilm on the opposite side. This results to minimization of light limitation and enhancement of CO_2 mass transfer between the cells and the ambient gas phase in PSBR systems. In both porous and non-porous biofilm configurations, the bulk of the culture media is separated from the

biomass. Thus, biomass can be easily scraped off from the substrate and can achieve final biomass values comparable to post-centrifuged harvest from suspension cultures[22,23].

Biofilm cultivation is an attractive strategy for marine benthic diatom cultivation. Benthic diatoms are biofilm formers in nature, developing large-scale cohesive assemblages with other microorganisms. This is demonstrated by their preference for minimally disturbed conditions. Although some marine diatom species thrive in an airlift PBR, other benthic species produced higher biomass productivity and lipid rate when they were grown undisturbed in Erlenmeyer flasks[24].

Benthic diatoms colonies greatly benefit from higher surface areas with marginal perturbation. The failure of certain species to grow in suspension leads to a potential re-evaluation of their eco-physiology and lipid production capacity under more favorable culture conditions using a biofilm photobioreactor. Research studies have shown great potential in cultivating microalgae using biofilm-based PBRs. However, since the conception of PSBR in 2002 and its successful lab-scale use on six benthic diatoms in 2005[25,26], the application of PSBRs for benthic diatoms studies remains scarce up to this day[27–30]. The development and utilization of a highly controlled biofilm system could potentially enhance the growth of benthic diatoms, improve their lipid production, and valorize their bioactivities for biopharmaceuticals.

In this study, a comparative analysis for the benthic marine diatoms strain *Amphora* sp. NCC169 cultivation was conducted between (a) Fernbach flask corresponding to batch culture and (b) a vertical, tubular lab-scale biofilm PSBR corresponding to continuous culture, both allowing the natural development of biofilm. The objective of this study is to estimate if under more highly controlled conditions in the biofilm PSBR, *Amphora* sp. NCC169 biomass and lipid yield is higher than those obtained from Fernbach flasks. To reach this goal, biomass, total lipid, and nutrient assimilation were investigated between culture conditions to determine optimum conditions towards high-value lipid production.

2. Materials and Methods

2.1. Strain and stock cultivation

Amphora sp. NCC169 is a strain of marine benthic diatom isolated from sediment samples

collected from the French Atlantic coast, near to Piriac-sur-Mer (47°22'06"N/02°32'52"W) in 2005. It was hosted by the Nantes Culture Collection (NCC) in Nantes University, France. It is currently contained within the Roscoff Culture Collection (RCC) under an updated species code RCC5813.

Stock cultures are grown under controlled conditions in 250-mL Erlenmeyer flasks containing 150 mL of natural seawater enriched with Guillard's F/2 culture medium[31]. Natural seawater was strained through a 0.2 µm membrane filter to remove particulates and most of the biological contaminants. Salinity was adjusted to 28 by dilution with demineralized or distilled water, while pH was set to 7.8 using hydrochloric acid or sodium hydroxide. The solution was sterilized by autoclaving at 121 °C (14.5 psi) for 20 minutes. After cooling down, the solution was infused with heat-labile nutrients and inoculated with *Amphora* sp. NCC169 cells under axenic conditions.

After inoculation, *Amphora* sp. NCC169 is grown in culture chamber under continuous lighting (24-hour photoperiod) at 150 µmoles $m^{-2}s^{-1}$ and at 16.8 ± 0.3 °C. Stock cultures are sub-cultured every month to ensure continuous supply of healthy cells.

2.2. Fernbach experiment

Amphora sp. NCC169 was cultured in Fernbach flasks with higher surface area/volume ratio (S/V) (28.4 m^2 m^{-3}) than conventional 250-mL Erlenmeyer flasks (17.7–20.1 m^2 m^{-3}) used in laboratory stock cultures. The Fernbach flasks were filled with 800 mL of natural seawater added with Guillard's F/2 medium, submerging the resulting biofilm under 5 cm of enriched seawaterEnrichment and sterilization of culture media in Fernbach flasks follow the same protocol as those in stock Erlenmeyer flasks. Cells were sub-cultured from the stock at a starting density of 30,000 cells·mL^{-1}. Cultures were kept at constant temperature (16.8 ± 0.3 °C), light intensity (150 µmoles $m^{-2}s^{-1}$), under continuous light.

Harvesting of biomass, estimating growth parameters, and analyzing of nutrients, total lipid content, fatty acids profile and pigments composition were performed every sampling period (day 2, 4, 6, 8, 10, 12, 14, 17, 20). In order to maintain the integrity of the biofilm throughout the culture period, one unit of Fernbach flask is allocated for every sampling day. The experiment was carried out in three

trials for day 0 to day 8, and six trials for day 10 to 20.

2.2.1 Cell health and density

To initiate sampling, biofilms formed on the bottom surface of the Fernbach flask were carefully dislodged using a magnetic stirrer for two minutes until cell aggregates are disrupted, and the solution is homogenized.

A 1-mL aliquot from the homogenized culture solution was used to measure the health of the cells using Pulse Amplitude Modulated (PAM) fluorometry (Walz GmbH, Effeltrich, Germany) in the cuvette version. The aliquot was initially dark-adapted at room temperature for 15 minutes, then pipetted into a 15-mm diameter quartz glass cuvette. The minimum fluorescence (F_0) was measured with a pulse of low level non-actinic measuring light, followed by a saturating light pulse (2500 µmol photons $m^{-2} \cdot s^{-1}$ for 0.8 s) to obtain the maximum fluorescence (F_m) value. The variable fluorescence yield (F_m - F_0) was then used to calculate the maximum photosystem II (PSII) quantum yield (F_v/F_m) of the dark-adapted sample (Eq. 1).

$$\frac{F_v}{F_m} = \frac{(F_m - F_0)}{F_m} \qquad \text{Eq. 1}$$

The health of the photosynthetic cells is proportional to the F_v/F_m, with the optimum value set between 0.5–0.7 for diatoms[32 33].

The same aliquot was used to measure the culture cell density (cells mL^{-1}) using a Neubauer hemocytometer and a light optical microscope (OLYMPUS CH40, Japan, objective Olympus ×20). The relative growth rate μ was calculated according to the following equation,

$$\mu = \frac{ln\,(N_t/N_0)}{\Delta t} \qquad \text{Eq. 2}$$

where N_0 is the population size at the beginning of the time interval (*i.e.* at t_0), N_t is the density at the end of the time interval (*i.e.* at t_t), and Δt is the difference between the time intervals ($t_t - t_0$)[34].

2.2.2 Biomass

The culture solution was harvested by filtering the cells through pre-combusted and pre-weighed glass microfiber filters (Whatman™ GF/F, ⌀ 47 mm, 0.7 µm pore size). Filtered diatom biomass was washed with ammonium formate (68 g·L^{-1}) to remove residual salt. Wet filters were frozen (-80 °C) and freeze-dried prior to dry weight estimation. Culture media samples were collected prior to the inoculation and before pre-treatment of ammonium formate for further nutrient analysis.

Total dry biomass was transformed to areal productivity corresponding to the bottom surface area of the Fernbach flask over time. Thus, biomass productivity ($P_{biomass}$) was calculated by Eq. 3,

$$P_{biomass} = m_{biomass} / A / t \quad \text{Eq. 3}$$

where $m_{biomass}$ is the final dry weight (g) of *Amphora* sp. NCC169 during one sampling point, A is the area of the bottom of the Fernbach flask (0.03 m^2), and t is the culture duration (day).

2.2.3. Total lipid and nutrient analysis

Total lipid (TL) were extracted following the modified Bligh and Dyer method[35]. The disks were pooled in solvent extraction composed by dichloromethane and methanol (1:1 ratio) into a flask, and mechanically agitated for 1 h. The solvent extract was filtered through a Whatman phase separating filter paper (⌀15.0 cm) to remove silica and other solid particulates resulting from the initial extraction, and subsequently added with water. The organic phase was purified using sodium sulfate and filtered for rotary evaporation. Total lipid was re-suspended on a small volume of dichloromethane and transferred into a pre-weighed vial. The residual dichloromethane was evaporated to obtain the total lipid extract by gravimetry. Final yield was expressed in percentage of the total dry weight. Total lipid productivity ($P_{total\ lipid}$) was expressed as g·m^{-2}·day^{-1} using the formula:

$$P_{total\ lipid} = m_{total\ lipid} / A / t \quad \text{Eq. 4}$$

where $m_{total\ lipid}$ is the total lipid weight (g) of *Amphora* sp. NCC169 during one sampling point, A is

the area of the bottom of the Fernbach flask (0.03 m^2), and t is the culture duration (day).

Water samples were taken for each sampling period to determine the nutrients present in the culture media. Continuous flow injection colorimetry was performed using SEAL Analytics AA3 HR2 Autoanalyzer to measure nitrate + nitrite (NO_3^- + NO_2^-), phosphate (PO_4^{3-}), and silicate (SiO_4^{4-}) (SEAL Analytical GmbH, Nordestedt, Germany)[36]. Nitrates are initially reduced to nitrites by passing the sample through a copper-treated cadmium column. The transformed nitrites, along with the pre-existing nitrites in the medium, react with sulphanilamide and *N*-naphthylethylenediamine to give a pink coloration measured at 540 nm. Phosphate and silicate ions react with molybdate to form a phosphomolybdic and β-silicomolybdic complex, respectively. These complexes are reduced by ascorbic acid to a blue compound measured at 820 nm. Ammonium (NH_4^+) levels were tested using Jasco® FP-2020 fluorometer with ADA (Seal Analytical) interface and analyzed using AACE® operating software. The method is based on the reaction of ammonium with orthophthaldialdehyde in the presence of a reducing agent in a slightly basic medium[36]. The fluorimetric analysis is performed at an excitation wavelength of 365 nm and an emission wavelength of 425 nm. The limits of quantification for these compounds are 0.2 µM (NO_3^- + NO_2^-), 0.06 µM (PO_4^{3-}), 0.04 µM (SiO_4^{4-}), and 0.05 µM (NH_4^+).

2.3. Porous substrate photobioreactor (PSBR) experiment

2.3.1 PSBR configuration

The PSBR used in this study is an adapted configuration for biofilm cultivation from previous designs. An existing commercial suspension PBR developed by Synoxis Algae® (Le Cellier, France)

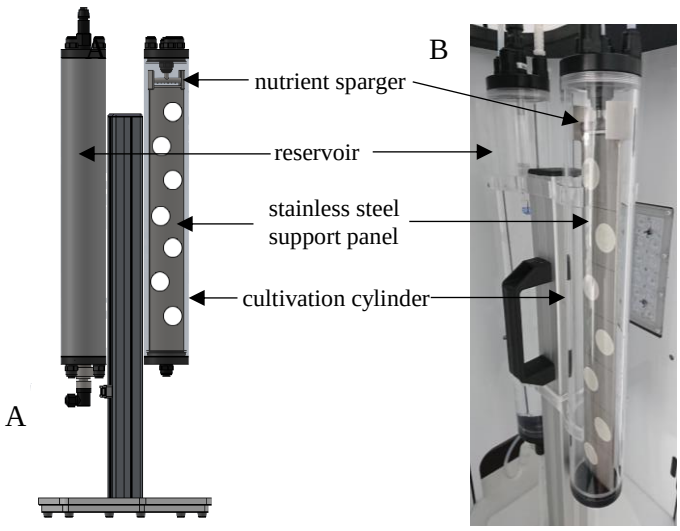

Figure 1 PSBR setup, adapted from an existing PBR for suspension cultivation, and currently composed of the cultivation (left) with steel panel covered by a lens tissue and supporting filters inoculated by diatoms; and the reservoir (right) cylinders (A)

called 'Nano' was adapted to build a PSBR system (Figure 1). The adapted PSBR is composed of two cylindrical culture and reservoir chambers, and a fiberglass compartment internally embedded with two LED technology panels with three different combination of wavelengths, λ (λ_{blue} = 469 nm + 449 nm, $\lambda_{green/orange}$ = 515 nm + 598 nm, λ_{red} = 633 nm + 654 nm). This setup is completed by a central control system that programs and automatically regulates pH, light, temperature, gas, and nutrient flow using an interactive touch screen. PSBR features and accessories illustrations are available as supplemental data (S1).

The setup is composed of two hollow vertically-oriented transparent poly(methyl methacrylate) (PMMA) cylinders assembled on a PMMA stand. The cylinders both have the same height (40 cm) and diameter (inner diameter = 5.1 cm; outer diameter = 5.9 cm).

The top cap for the main culture cylinder is installed with male union fittings to suspend the removable T-shaped stainless steel sparger consisting of eight equidistant ⌀1-mm diffuser holes. During culture, a sheet of lens cleaning tissue (Whatman, Catalog Number: 2105-918) is placed over the steel panel and serves as a source layer to establish the flow of the culture media. The culture medium is distributed on the tapered top edge of the metal panel and trickles further onto the lens paper. The liquid gets distributed to the glass fiber filter disk by absorption and gravity. The amount of culture medium flowing through and out of the biofilm photobioreactor is regulated by several peristaltic pumps in the control unit.

Circular glass fiber filters (Whatman™ GF/C ⌀25 mm, 0.7 µm pore size) were placed onto the source layer to act as self-adhesive substrate layer for the immobilized benthic diatoms. The substrate layer allows the passage of culture medium from the source layer into the biomass while preventing the reverse migration of the cells to the source layer and the culture medium.

2.3.2 Inoculation

Pre-combusted (400 °C, 4 h) GF/C filter disks (⌀25 mm, 0.7 µm pore size) were used as substrate for the diatom biofilm. Individual filter disks were placed inside a 6-well cell culture plate and inoculated with a total of 1 million cells of *Amphora* sp. NCC169. The cells were carefully inoculated

on the surface of the filter disks to prevent growth initiating on the underside of the disks. An additional volume of natural seawater enriched with Guillard's F/2 medium was added into each cell well to reach a final volume of 2 mL. Inundation of F/2 medium was done slowly and carefully so as not to displace the diatom cells on the surface of the disks. The disks were left to incubate in the culture room (temperature = 17.6 ± 2.1 °C, light regime/intensity = continuous; 150 µmoles m^{-2} s^{-1}) until a stable biofilm is formed after three days. Five culture plates were prepared to ensure biofilm colonization on at least 14 GF/C filter disks.

2.3.3 PSBR launch

During culture, the panel was outlined with a grid to set seven disks approximately 5 mm horizontally away from each other. The same number of disks are similarly positioned on the other side of the panel for a total of 14 disks. Continuous light was provided by two panels of RGB LED channels set at a global intensity of 150 µmoles m^{-2} s^{-1}, while external temperature was maintained at 17.6 ± 2.1 °C.

2.3.3 Sampling measurements

Growth estimation of immobilized cells in the PSBR was not possible using conventional cell counting techniques for several reasons. The developed design for the PSBR doesn't allow for sampling without opening the chambers and potentially introducing contaminants into the system. A single lab-scale photobioreactor doesn't have enough facility for multiple samplings. In the end, we have decided to sample twice—on day 0 and day 7, coinciding with the general late exponential phase of *Amphora* sp. NCC169 in the previous Fernbach experiments.

The biomass of the biofilm formed on the filter disks was measured non-destructively using normalized difference vegetation index (NDVI)[10]. NDVI is frequently used to evaluate the biomass of terrestrial vegetation, as well as to measure biofilm and microphytobenthos growth using satellite data[37–40]. The reflectance (ρ) of the cells at certain wavelengths are known to be proportional to their chlorophyll *a* content and is used as reliable proxy for biomass. For each disk, 10 global reflectance values were taken at different representative points using Ocean Optics Flame-UV-S-VIS-

NIR-ES miniature spectroradiometer. The reflectance values at the maximal reflectance wavelength (λ750) and the chlorophyll *a* absorption wavelength (λ675) were used to calculate the NDVI (Eq. 5). An average of 10 NDVI values were obtained for each disk every sampling period to account for potential heterogeneity.

$$NDVI = \frac{\lambda_{750} - \lambda_{675}}{\lambda_{750} + \lambda_{675}} \quad \text{Eq. 5}$$

The physiological stress and photosynthetic activity of the biofilms were measured through pulse-amplitude modulated (PAM) fluorometry (Walz GmbH, Effeltrich, Germany), but using the optical fiber version[41,42]. Similar to the Fernbach experiment, low level non-actinic measuring light was initially applied to dark-adapted (15 minutes) samples to get the minimum fluorescence yield (F_0), followed by a strong saturating pulse to reach the maximum fluorescence level (F_m) to calculate the maximum quantum efficiency (F_v/F_m) parameters (Eq. 1). Three F_v/F_m values were sampled at different points to estimate the diatoms' physiological stress and photosynthetic efficiency.

Three seven-day trials were conducted using the PSBR. At the end of the culture cycle, all the algal disks were harvested from the biofilm photobioreactor. The biomass and photosynthetic activity of the films were measured similar to the protocol in the beginning of the experiment. The disks were individually washed with ammonium formate (68 g·L^{-1}), frozen at -80 °C, and lyophilized to a constant weight. Dry biomass estimation, lipid extraction, and nutrient analyses were done as in the Fernbach experiment.

2.4. Statistical analysis

Data obtained from the experiments both using Fernbach flasks and PSBR were expressed as mean ± standard deviation. Test for statistical significance was performed through the PAleontological STatistics (PAST) software (version 4.08). The values were evaluated for normality using the Shapiro–Wilk *W* test. Student's independent *t*-test was used to compare the means between two groups. For groups of three or more, analysis of variance (ANOVA) was used if the data was normally distributed. Percentage data of total lipid was transformed when necessary[43]. However, Kruskal-

Wallis was used if the assumptions of the normal distribution were violated. *Post hoc* Tukey HSD tests were used to verify the individual differences of normally distributed datasets, while Mann-Whitney U test was used otherwise.

3. Results and discussion

3.1. Fernbach flasks

In Fernbach flasks, the initial biomass density was 3.6 x 10^4 cells·mL^{-1} and gradually increased to 1.43 x 10^4 cells·mL^{-1} after 20 days of culture (Figure 2). The sigmoid growth curve does not have a prominent lag phase. There was a plateau in cell density from day 3 to day 14, following by an increase in days 18 and 20, but without any significantly difference (Tukey HSD test, $p > 0.05$). The highest growth rate was achieved between day 2 and day 4 at 0.8 ± 0.4 day^{-1}. But, average growth rate of *Amphora* sp. NCC 169 between sampling periods was 0.2 ± 0.1 day^{-1} which is comparable with the studies conducted by de la Peña (2007)[44] on culturing *Amphora* sp. in the laboratory, reaching 0.2 ± 0.1 day^{-1}, and Indrayani et al. (2019) on *Amphora* sp. MUR258 in outdoor raceway ponds reaching 0.29 day^{-1}[45].

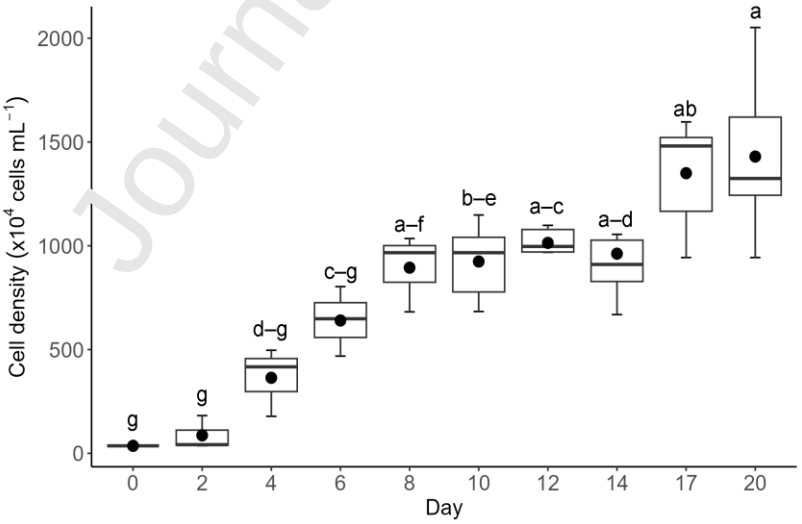

Figure 2 Box plot distribution of the average cell density across different cultivation periods using Fernbach (Day 0-8 n=3; Day 10-20 n=6). Error bars represent minimum and maximum values, whereas rectangle boundaries represent the 1st and 3rd quartile values separated by the median. Mean values were plotted as black-filled circles (●). Letters on top of error bars indicate significance of means at the 0.05 level according to an HSD test. Mean cell densities denoted by a different letter or range of letters indicate significant differences between treatments (Tukey HSD, $p < 0.05$).

The photosynthetic efficiency (F_v/F_m) of the cells remained high from day 0 to day 17 with an average value of 0.5 ± 0.1 (Tukey HSD test, p > 0.5), and then gradually decreased to 0.3 ± 0.1 (Tukey HSD test, Q = 5.60, p = 0.02) (Figure 3).

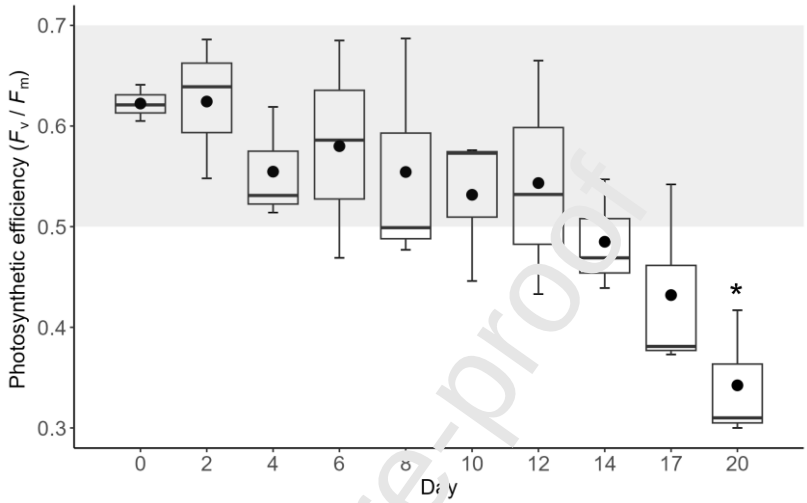

Figure 3 Variation of the average photosynthetic efficiency (F_v/F_m) of *Amphora* sp. NCC169 in Fernbach flasks over time (n=3). Error bars represent minimum and maximum values, whereas rectangle boundaries represent the 1st and 3rd quartile values separated by the median. Black-filled circles (●) represent the mean F_v/F_m of each sampling period. The optimum range of photosynthetic efficiency for diatoms (0.5–0.7) is highlighted in gray. Error bars with asterisk (*) indicate significance (Tukey HSD, $p < 0.05$)

Total dry biomass (mg) and the total lipid (% dry weight) of *Amphora* sp. NCC 169 were directly proportional with time (Figure 4). Highest recorded value for total dry biomass was obtained on the last days of culture reached up to 158 mg (Day 17 and 20: Tukey HSD test, Q = 2.53, p = 0.69). Even if the total lipid reached 24.4 ± 5.6% on day 20, it remained stable from day 8 to day 20 with an average value of 20.4 ± 4.9% (Tukey HSD test, p > 0.05). When compared to previous study in Erlenmeyer flasks[10], the total lipid ratio of *Amphora* sp. NCC169 cells obtained after 13 ± 3 days (16.0 ± 2.6%) in Erlenmeyer flasks Fernbach flasks was reached after only eight days (16.2 ± 5.3%) in Fernbach flasks. By day 14, Fernbach cultures had 56% more total lipid than those in the Erlenmeyer flasks.

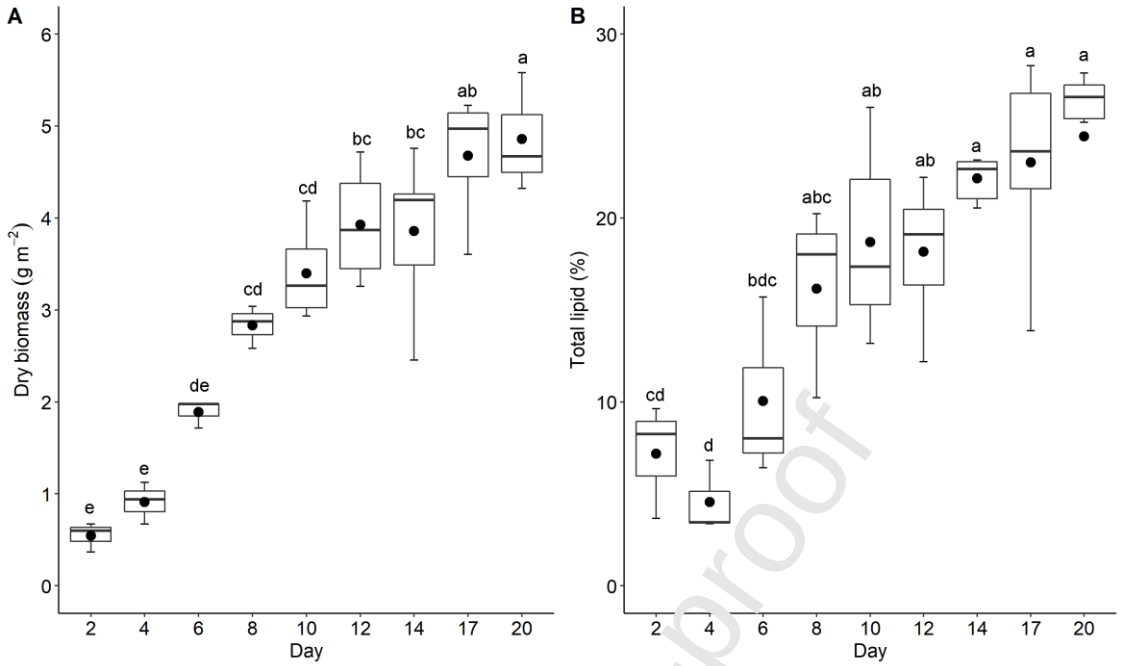

Figure 4 Box plot distribution of the average dry biomass density and total lipid rate of *Amphora* sp. NCC169 in Fernbach flasks across different cultivation periods (Day 0-8 n=3; Day 10-20 n=6). Error bars represent minimum and maximum values, whereas rectangle boundaries represent the 1st and 3rd quartile values separated by the median. Mean values were plotted as black-filled circles (●). Letters on top of error bars indicate significance of means according to an HSD test. Mean cell densities denoted by a different letter or range of letters indicate significant differences between treatments (Tukey HSD, $p < 0.05$).

The biomass and lipid productivities of *Amphora* sp. NCC169 in Fernbach flasks were expressed as a function of area over time ($g \cdot m^{-2} \cdot day^{-1}$) to make quantitative comparisons with the PSBR, as well as to follow the common productivity growth metrics in literature (Figure 5)[29]. During 20 days of culture, the biomass productivity remained stable with an average of 0.30 ± 0.04 $g \cdot m^{-2} \cdot day^{-1}$ (Tukey HSD, $p > 0.05$). This value is comparatively lower than what was previously achieved in 250-mL Erlenmeyer flasks after 13 ± 3 days (75 ± 3.9 $mg \cdot L^{-1} \cdot day^{-1}$)[10]. In this cited study, the best diatom growth rates were given by *Entomoneis paludosa* (14.4–329.6 $mg \cdot L^{-1} \cdot day^{-1}$), *Craspedostauros* spp. (120.6–265.5 $mg \cdot L^{-1} \cdot day^{-1}$), *Staurosira* sp. (244.3 $mg \cdot L^{-1} \cdot day^{-1}$), *Fallacia* spp. (174.6–238.0 $mg \cdot L^{-1} \cdot day^{-1}$), *Surirella* sp. (193.2 $mg \cdot L^{-1} \cdot day^{-1}$), (*Amphora* sp. 137 $mg \cdot L^{-1} \cdot day^{-1}$), *Brockmaniella* sp. (133.6 $mg \cdot L^{-1} \cdot day^{-1}$), *Extubocellulus* sp. (127.4 $mg \cdot L^{-1} \cdot day^{-1}$), and *Contricriba weissflogii* (126.1 $mg \cdot L^{-1} \cdot day^{-1}$).

Lipid productivities were significantly higher on days 8–20 (Tukey HSD, $p \leq 0.05$), peaking at 0.1 ± 0.0 $g \cdot m^{-2} \cdot day^{-1}$ after 20 days.

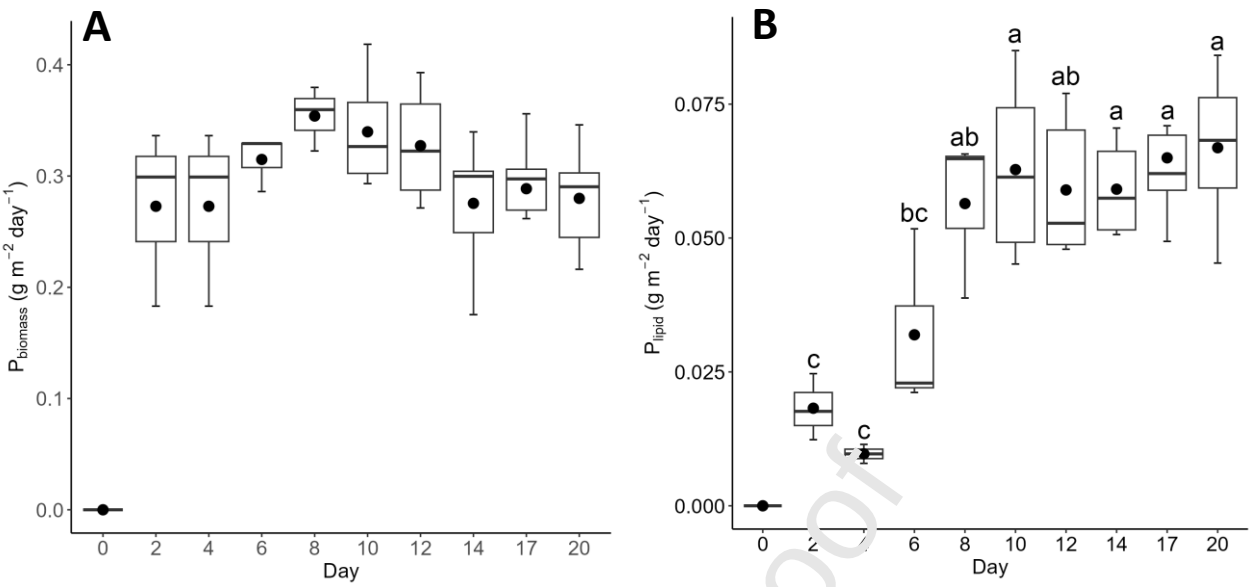

Figure 5 Average biomass (A) and lipid (B) productivities (in g m^{-2} day^{-1}) of *Amphora* sp. NCC169 over 10 different culture periods. Error bars represent minimum and maximum values, whereas rectangle boundaries represent the 1st and 3rd quartile values separated by the median. Black-filled circles (●) represent the mean productivity of the respective sampling periods. Letters on top of error bars indicate significance of means according to an HSD test. Mean cell densities denoted by a different letter or range of letters indicate significant differences between treatments (Tukey HSD, $p < 0.05$).

The evolution of main macronutrients (nitrate + nitrite, silicate, and phosphate) as well as ammonium levels were investigated (Figure 6). All of the nutrients experienced a visible downward trend, as expected of batch cultivation systems. Nitrate and nitrite values significantly decreased by 63.8 ± 1.4% from its original concentration on the fourth day of culture (Tukey HSD test, Q = 6.26, p = 0.07). Silicate levels were significantly 83.6 ± 11.7% lower than their original concentration by day 6 (Tukey HSD test, Q = 5.47, p = 0.02), and was further reduced 0.9 ± 0.8% of their original concentrations by the end of the culture period (Tukey HSD test, Q = 5.99, p = 0.01). On the other hand, average phosphate concentrations remained stable during the culture (ANOVA, F = 1.32, p = 0.29). Ammonium levels fluctuated between 0.6 ± 0.6 µM to 5.0 ± 2.8 µM, but observed changes were not statistically significant (Tukey HSD test $p > 0.05$).

The higher surface area/volume (S/V) ratio in Fernbach flasks did not translate to better biomass growth and productivity for *Amphora* sp. NCC169. The decrease in growth rate and biomass productivity is a likely implication of photoinhibition, as more cells are spread out over a higher surface and thus exposed to high irradiances[46]. Cellular activities that depend on the input of light energy (e.g., nutrient consumption, CO_2 absorption) take place at a higher rate, which could have long-

term detrimental effects to the growth and productivity of the cells. For example, higher photosynthetic activity without CO_2 supplementation increases the pH value, which may inhibit metabolism[47,48]. This is supported by the deterioration of the photosynthetic efficiency of *Amphora* sp. NCC169 in Fernbach flasks from day 14 onwards, which coincides with the decline of F_v/F_m values below the optimum threshold of 0.5 – 0.7. Furthermore, progressive pigment analysis suggests direct correlation between chlorophyll a levels and F_v/F_m values [39].

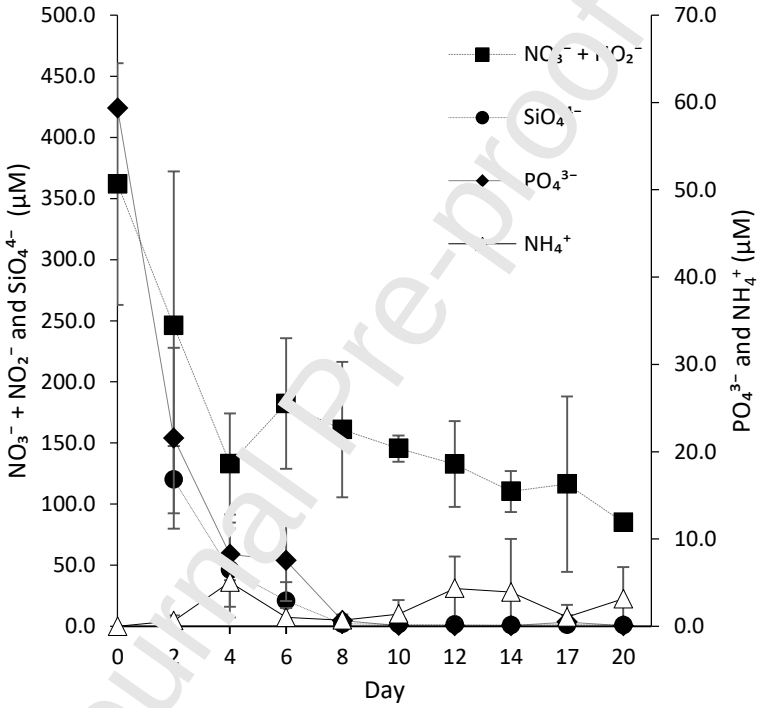

Figure 6 Average nutrient availability (NO_3^- + NO_2^-, PO_4^{3-}, SiO_4^{4-}, and NH_4^+) in Fernbach flasks culture media at every sampling interval (except for SiO_4^{4-} without day 0). Error bars represent standard deviation (n = 3).

3.2 PSBR

Amphora sp. NCC169 formed dense, unialgal biofilms that cover the inoculated area after seven days (Figure 7).

Figure 7 Photographic comparison of biofilm disks inoculated on the left side and right side of the PSBR support panel on the day of launch (Day 0) and after harvest (Day 7).

The culture panel supports healthy cells, as reflected by the F_v/F_m values never fall within the optimum threshold (Figure 8A), whatever the side used (Tukey HSD test, Q = 1.18, p = 0.41), and despite a small decrease on the final day (Tukey HSD test, Q = 4.12, $p < 0.01$). Additional pigment content investigation could elucidate the optimum S/V ratio for *Amphora* sp. NCC169 as a function of light availability at a given algal physiological state. This will enable simulations and modelling of biomass and lipid productivity, as well as optimization for subsequent scale-up technologies.

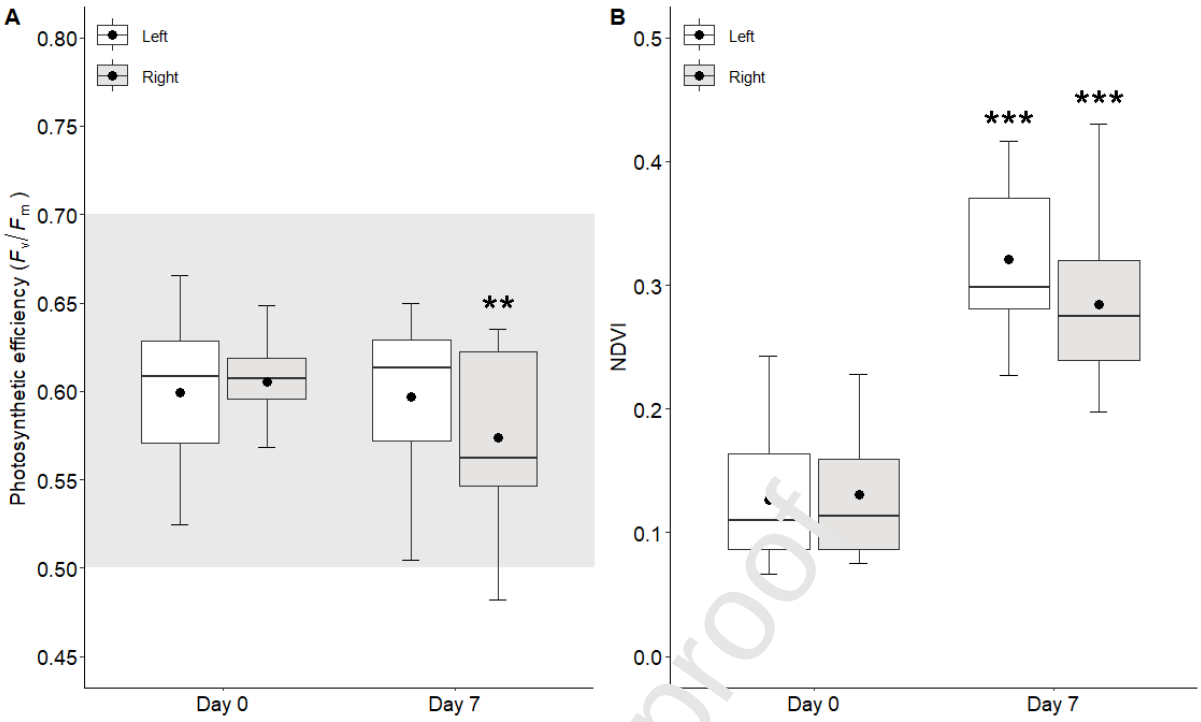

Figure 8 Average photosynthetic efficiency (F_v/F_m) (A) and NDVI (B) of *Amphora* sp. NCC169 biofilm disks in the PSBR (n = 21). Data is categorized between the location of the disks on the support panel (left and right), and sampling period (day 0 and day 7). The median line separates the 1st and 3rd quartile rectangle boundaries, while error bars represent minimum and maximum values. Black-filled circles (●) represent the population mean. The optimum range of photosynthetic efficiency for diatoms (0.5–0.7) is highlighted in gray. Asterisks show significant difference at *$p < 0.05$, **$p < 0.01$, or ***$p < 0.001$ (Tukey HSD).

NDVI values significantly increased from day 0 (left = 0.13 ± 0.06; right = 0.13 ± 0.06) to day 7 (left = 0.35 ± 0.07; right = 0.33 ± 0.06) without any effect due to the used side (Tukey HSD test, Q = 15.75, $p < 0.001$) (Figure 8B). This growth is further illustrated by the increase in biofilm color intensity on the day of harvest (Figure 7). NDVI values have high standard deviations that reflect the patchy biofilm development. However, data analysis shows that this heterogeneity is not significant (Tukey HSD test, Q = 0.60, $p = 0.67$).

After seven days of culture, both sides of the support panel have shown similar average pooled dry biomass reaching 11.5 ± 1.7 mg on the left side and 11.0 ± 3.0 mg on the right (Figure 9, $t = 0.07$, $p = 0.95$). Mean total lipid rate was also similar for both sides, reaching 22.0 ± 5.2% and 18.2 ± 4.5% for the left and right side, respectively ($t(4) = 0.96$, $p = 0.39$).

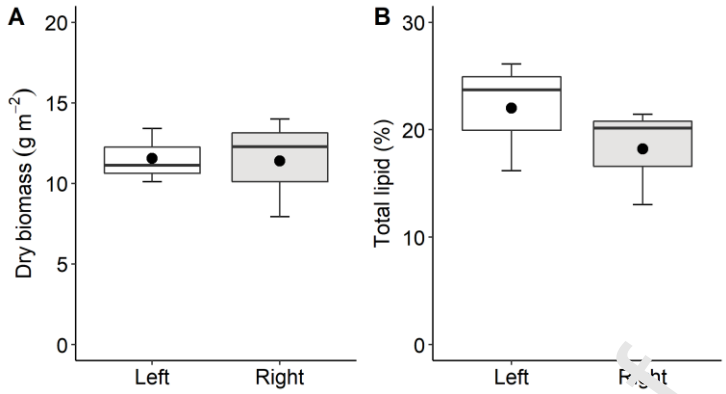

Figure 9 Box plot distribution of the average dry biomass density and total lipid content in percent dry biomass of *Amphora* sp. NCC169 on disks located on the left and right side of the PSBR upon harvest (day 7, n=6). Error bars represent minimum and maximum values, whereas rectangle boundaries represent the 1st and 3rd quartile values separated by the median. Mean values were plotted as black-filled circles (●).

Silicate and nitrate/nitrite decreased by 21% (day 0 = 68.32 µM; day 7 = 53.79) and 25% (day 0 = 643.73 µM; day 7 = 483.60 µM) after seven days, respectively (Figure 10). On the other hand, phosphate decreased to 24% of the original concentration (day 0 = 59.35 µM; day 7 = 14.01 µM), and ammonium to 10% (day 0 = 168.98 µM, day 7 = 16.87 µM), showing the highest consumption rate among the main macronutrients, even if the change in nutrient concentration in the culture medium is not statistically significant (Mann- Whitney, U = 3, $p > 0.05$).

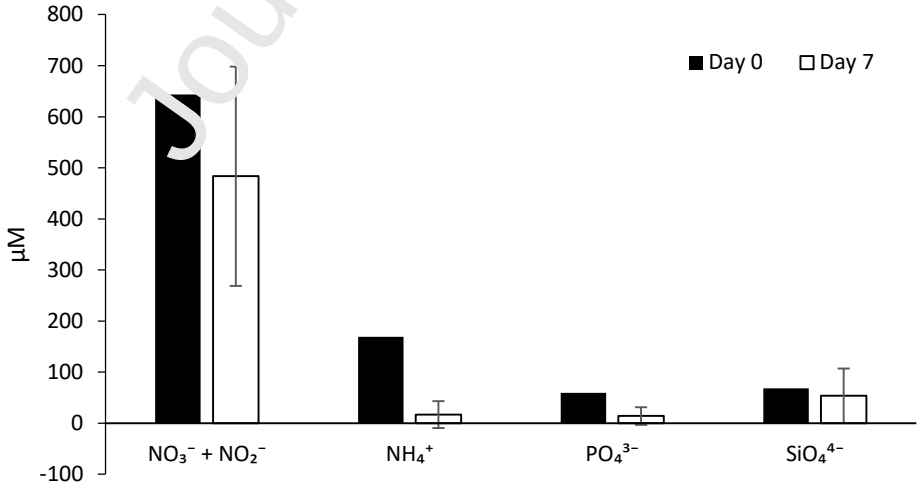

Figure 10 Nutrient analysis of *Amphora* sp. NCC169 grown in PSBR. Error bars represent standard deviation of replicates (n=3). Day 0 doesn't have replicates.

3.3 Productivity comparison between Fernbach and PSBR cultures

The PSBR has a dry biomass productivity of 0.5 ± 0.1 g m^{-2} day^{-1} after seven days of culture, which is statistically higher than the biomass productivity achieved by the Fernbach cultures at any sampling

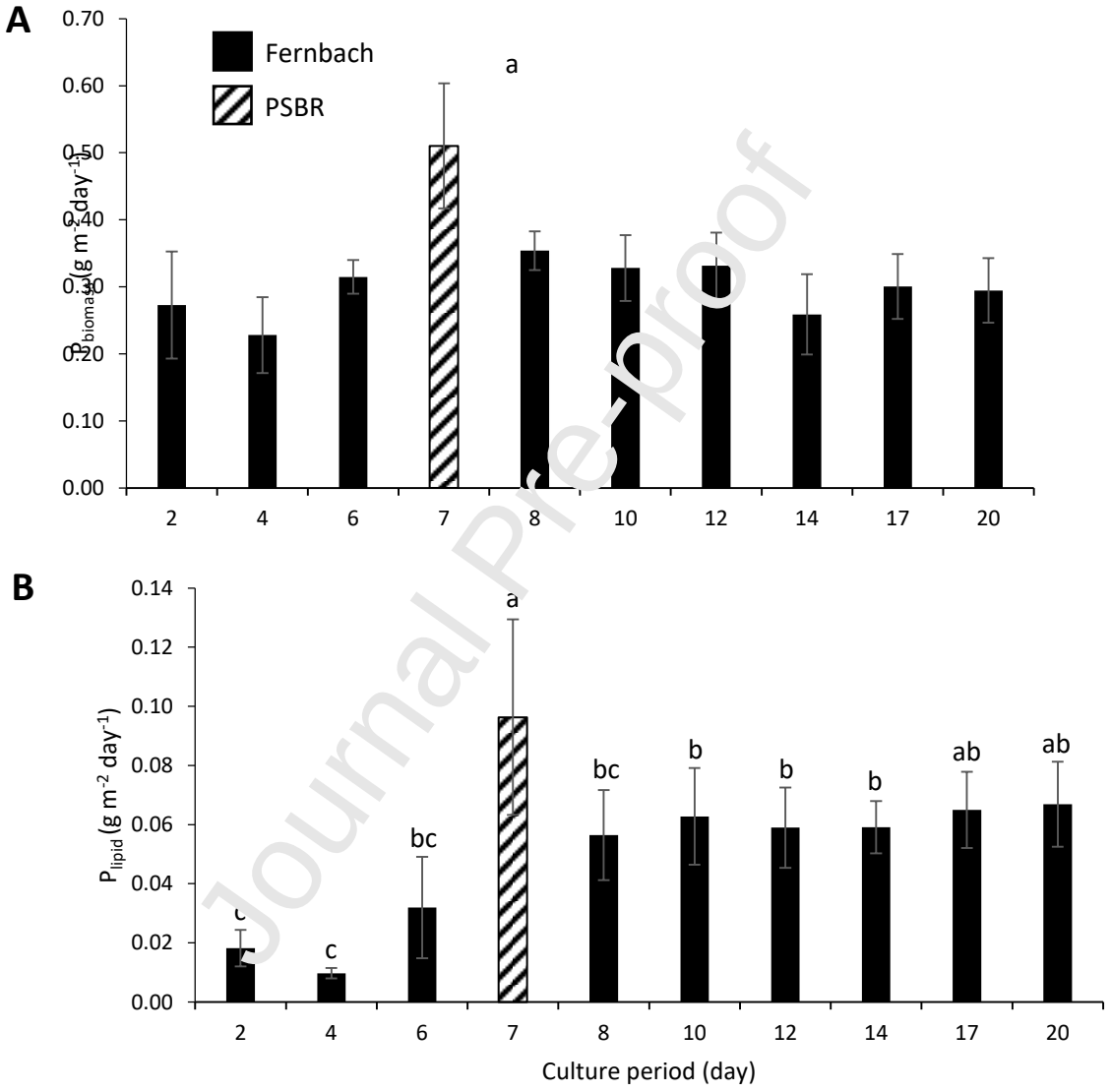

Figure 11 Average biomass (A) and lipid productivity (g m^{-2} day^{-1}) (B) of *Amphora* sp. NCC169 cultured in Fernbach flasks and in a PSBR. Error bars represent the standard deviation of the mean (n = 3 to 6). Letters represent treatment that have statistically significant difference in means (Tukey HSD test, $p \leq 0.05$). Values with the same letter are not significantly different ($p > 0.05$).

point (Tukey HSD test, $p \leq 0.05$) (Figure 11A).

This supports the result of previous studies showing that attached microalgae cultivation systems are more productive than suspension methods[49,50]. The surface biomass productivity of attached

cultivation methods reported in the literature ranges between 0.04 – 80 g m^{-2} day^{-1}, depending on the influence of different factors (e.g., species, nutrient levels, temperature, light intensity, culture scale, attachment material)[22,50]. Algae species with negative free energy of cohesion (e.g., *Ankistrodesmus falcatus*, *Botryococcus braunii*, *Botryococcus sudeticus*, *Cylindrotheca fusiformis*) indicate better adhesion to artificial substrates because of their dominating attractive acid-base and van der Waals interaction[51]. This determines the hydrophobicity of the cells and their superiority in forming biofilms. Additionally, the magnitude of algae-surface interactions is directly proportional to cell size. Higher algal diameters denote higher attractive or repulsive forces. However, the influence of lift and drag forces of fluid flow must be considered in order to promote optimized adhesion of the algal cells. For example, flow rate was shown to have significantly reduced the net force acting on an adhered cell, decreasing the effective cell diameter from 10.4 to 4.3 µm[51].

The highest recorded surface biomass productivities across different modes of attached cultivation were indeed dominated by green algae (*Scenedesmus obliquus* 50-80 g m^{-2} day^{-1}; *Halochlorella rubescens* 31 g m^{-2} day^{-1}; *Chlorella sorokiniana* 20.1 g m^{-2} day^{-1})[22,52]. However, this could be owing to the fact that attached cultivation systems have thus far been primarily used for planktonic green algae. Benthic diatoms have the advantage to thrive in attached cultivation systems because of their ubiquitous biofilm-forming capacity[53,54]. Although some attached cultivation operations include diatom species like *Nitszchia* sp., *Cymbella* sp., *Melosira* sp., *Gomphonema* sp., *Synedra* sp., *Eunotia* sp., *Diatoma* sp. and *Navicula* sp., they're usually mixed in with other microalgae species[55–57]. Research on more diatom species under similar experimental conditions is necessary for more robust comparisons.

Biomass productivity of suspended cultures were often expressed as a function of volume, hence, data on biomass productivity of microalgae in flasks as expressed in g m^{-2} day^{-1} is still wanting. However, comparison is feasible by having the same culture volume, as in the case of *Chlorella* sp. where attached cultivation generated 36% more algal biomass than its suspension counterpart[23]. Comparative growth performance of mixed microalgae cells in raceway ponds revealed a 2.8-times higher algal biomass when the ponds were installed with attachment substrates[49].

The higher productivity values of *Amphora* sp. NCC169 immobilized in the PSBR could be due to

the higher mass-transfer efficiency of gases, nutrients, and light to support growth. In the PSBR, the biofilm cells have direct gas exchange and shorter light diffusion path through the thinner liquid membrane (PSBR = < 0.05 cm; Fernbach flask = 5 cm). This prevents the excessive accumulation of photosynthesis-generated oxygen in the biofilm, thereby reducing the negative effects of photoinhibition or photo-oxidation on net photosynthesis and keeping the F_v/F_m at optimum[58,59]. Biofilm cells can directly access and take up CO_2 from the gas phase [60]. On the other hand, in the Fernbach cultures, culture medium wasn't mixed during the period of cultivation. Hence, any available CO_2 is limiting as they must first diffuse through the gas-liquid interface prior to cellular uptake. This limitation was ameliorated using the PSBR where the biofilm cells are directly in contact with the ambient gas phase and continuous fresh supply of culture medium. Moreover, this setup allows for better light availability than suspension cultures.

As for biomass productivity, lipid productivity was significantly higher in the PSBR (0.1 ± 0.03 g m^{-2} day^{-1}) than in Fernbach cultures harvested before day 14 (Tukey HSD test, $p \leq 0.05$) (Figure 11B). However, lipid productivity of *Amphora* sp. NCC169 cultured in the PSBR after 7 days and those grown in the Fernbach flasks beyond day 10 (day 17 and 20) were similar (Tukey HSD test, $p > 0.05$).

In the PSBR, *Amphora* sp. NCC169 constantly maintained optimal photosynthetic efficiency until harvest. This reflects healthy metabolic status and minimal stress to the cells. As healthy biofilm thickens, cells become self-shaded and light limitation generally increases the F_v/F_m of low-light adapted benthic diatoms[63]. Furthermore, the dark regions contribute to the heterotrophication of the cells which subsequently foster cellular growth and lipid enrichment[62]. High lipid productivity is not directly proportional to high lipid quality. The first step in this study is to improve the biomass productivity of *Amphora* sp. NCC169 and sustain the cells in good health. Afterwards, optimization of lipid accumulation and lipid quality of the cells is imperative for species valorization. These can be improved under highly controlled conditions using the PSBR. Subsequent analysis of lipid fractions obtained from PSBR is needed to investigate the feasibility of producing high-quality lipids for biotechnological applications.

Although there has been a commonly observed downward trend of F_v/F_m in benthic diatoms under laboratory conditions[61], the decline in F_v/F_m is a potentially valuable indicator of nutrient starvation

and/or degree of photoinhibition[63–66]. In Fernbach flasks, macronutrient concentrations were significantly reduced by 68% (NO_3^- + NO_2^-) to as much as 99% (PO_4^{3-} and SiO_4^{4-}) at day 14. Although the Redfield-Brzezinski ratios in the culture media continue to fall within the acceptable threshold for diatoms (Si:N:P = 15:16:1)[67], the available concentrations of each macronutrient have significantly diminished at the end of the experimental period. The accumulation of several nutrient limitations (N and P) have been shown to strongly influence the F_v/F_m values of benthic diatoms *Entomoneis paludosa*, *Nitzschia alexandrina*, and *Staurosira* sp.[63]. As these compounds are highly precipitating with other molecules in seawater (e.g., Ca^{2+}, Mg^{2+}), the rapid decrease in media concentrations highlight subsequent enrichment to prevent any possible limitation in the system. A similar trend has been observed for the nutrients in an airlift culture of *Haslea ostrearia*, which was ameliorated by introducing a fed-batch strategy of HCO_3^-, PO_4^{3-} and SiO_3^{2-}[68]. Light stress introduced to the PSII system can also damage the photosynthetic apparatus, inhibit the light energy conversion, and eventually decrease the overall F_v/F_m [61,69]. Regardless, it has been shown that in nutrient-deficient conditions, the effect of light intensity on the PSII maximum efficiency of some species of marine benthic diatoms is negligible[63].The productivity of *Amphora* sp. NCC169 in the current PSBR is comparatively lower than the biomass productivities of other algal species using previously designed PSBRs[28,45]. This may be due to severe carbon limitation within the culture cylinder. Although the culture media reservoir was injected with CO_2 to stabilize the pH of the culture medium, the culture cylinder itself was left bereft, leaving gas exchange between the cells and the ambient air severely compromised. This could likewise explain the paltry difference in performance in comparison with the Fernbach flasks. The current PSBR design is a newly-adapted design from an existing suspension photobioreactor configuration, and not an exact replication of any of its predecessors. The PMMA cylinder that houses the support panel and reservoir were designed for planktonic algae, with which they are in direct contact. However, translated into a PSBR, this experimental adaptation still needs to undergo thorough simulation of engineering and species-specific biological factors to investigate the dynamic processes within the PSBR.

4. Conclusion and Perspective

Overall, porous substrate photobioreactor systems are promising in microalgae culture in general,

and benthic diatoms in particular. The use of the PSBR enabled *Amphora* sp. NCC169 to proliferate at higher biomass and lipid productivities than those cultivated in Fernbach flasks. The results obtained in this study set a benchmark towards identifying critical knowledge gaps in benthic diatom ecophysiology and attached cultivation research.

Optimization of the PSBR design is ongoing to improve the biomass and total lipid yield of *Amphora* sp. NCC169. Subsequent experiments will focus on the selection of the best substrate material and use the entire surface area of the support panel to obtain higher biomass yield. This will help in understanding surface physicochemical properties and determine substrate materials that promote superior biofilm characteristics for both lab-scale and commercial-scale cultivation. Additionally, choosing a durable and sustainable substrate for long-term biofilm operations is another important consideration.

Research will also have to assess the productivity of *Amphora* sp. NCC169 in the PSBR with respect to different light intensity and nutrient supply. Furthermore, the interactions between host-diatoms and their associated bacteria will be investigated in the PSBR setting to elucidate the important implications for overall diatom fitness. Most studies on bacteria-diatom co-cultures show positive influence on algal biomass by virtue of synthesized metabolites during cultivation that optimizes algal growth. Finally, life cycle analysis and overall operational costs will have to be investigated for future mass-production.

5. Acknowledgments

We are very grateful to the Pays de la Loire region (France) for financially supporting our research (via the SMIDAP grant BIOFILM, agreement n° 2021_04302). We would also like to acknowledge Synoxis Algae for the invaluable contribution to the development and engineering of the PSBR. We sincerely thank Ms. Clarisse Hubert from IFREMER (DG-ODE-PHYTOX-METALG) for her assistance in nutrient analyses of the samples and also Philippe Rosa and Alexandra Petit for their technical help in ISOMer lab.

6. References

[1] G.C. Underwood, J. Kromkamp, Primary production by phytoplankton and microphytobenthos in

estuaries, Adv. Ecol. Res. 29 (1999) 93–153.

[2] A.E. Allen, C.L. Dupont, M. Oborník, A. Horák, A. Nunes-Nesi, J.P. McCrow, H. Zheng, D.A. Johnson, H. Hu, A.R. Fernie, Evolution and metabolic significance of the urea cycle in photosynthetic diatoms, Nature. 473 (2011) 203–207.

[3] J.-K. Wang, M. Seibert, Prospects for commercial production of diatoms, Biotechnol. Biofuels. 10 (2017) 16.

[4] M.J. Furnas, In situ growth rates of marine phytoplankton: approaches to measurement, community and species growth rates, J. Plankton Res. 12 (1990) 1117–1151.

[5] J.-B. Lee, K. Hayashi, M. Hirata, E. Kuroda, E. Suzuki, Y. Kubo, T. Hayashi, Antiviral sulfated polysaccharide from *Navicula directa*, a diatom collected from deep-sea water in Toyama Bay, Biol. Pharm. Bull. 29 (2006) 2135–2139.

[6] S.K. Prestegard, L. Oftedal, R.T. Coyne, G. Nygaard, K.H. Skjærven, G. Knutsen, S.O. Døskeland, L. Herfindal, Marine benthic diatoms contain compounds able to induce leukemia cell death and modulate blood platelet activity, Mar. Drugs. 7 (2009) 605–623.

[7] P. Kroth, Molecular biology and the biotechnological potential of diatoms, in: Transgenic Microalgae Green Cell Factories, Springer, 2007: pp. 23–33.

[8] A. Bozarth, U.-G. Maier, S. Zauner, Diatoms in biotechnology: modern tools and applications, Appl. Microbiol. Biotechnol. 82 (2009) 195–201.

[9] P. Kuczynska, M. Jemiola-Rzeminska, K. Strzalka, Photosynthetic pigments in diatoms, Mar. Drugs. 13 (2015) 5847–5881.

[10] E. Cointet, G. Wielgosz-Collin, V. Méléder, O. Gonçalves, Lipids in benthic diatoms: A new suitable screening procedure, Algal Res. 39 (2019) 101425.

[11] O. Pulz, Photobioreactors: production systems for phototrophic microorganisms, Appl. Microbiol. Biotechnol. 57 (2001) 287–293.

[12] L. Xu, P.J. Weathers, X. Xiong, C. Liu, Microalgal bioreactors: challenges and opportunities, Eng. Life Sci. 9 (2009) 178–189.

[13] Y.R. Cruz, D. Aranda, P.R. Seidl, G.C. Diaz, R.G. Carliz, M.M. Fortes, D. da Ponte, R. de Paula, Cultivation systems of microalgae for the production of biofuels, in: Biofuels - State Dev., Intech

Open London, UK, 2018: pp. 199–218.

[14] A.S. Carlsson, J.B. van Beilen, R. Möller, D. Clayton, Micro-and macro-algae: utility for industrial applications: outputs from the EPOBIO project, CPL Press, University of York, 2007.

[15] W. Zhou, Q. Lu, P. Han, J. Li, Microalgae cultivation and photobioreactor design, in: Microalgae Cultiv. Biofuels Prod., Elsevier, 2020: pp. 31–50.

[16] T.J. Johnson, S. Katuwal, G.A. Anderson, L. Gu, R. Zhou, W.R. Gibbons, Photobioreactor cultivation strategies for microalgae and cyanobacteria, Biotechnol. Prog. 34 (2018) 811–827.

[17] S. Rezvani, I. Saadaoui, H. Al Jabri, N.R. Moheimani, Techno-economic modelling of high-value metabolites and secondary products from microalgae cultivated in closed photobioreactors with supplementary lighting, Algal Res. 65 (2022) 102733.

[18] S. Krichnavaruk, S. Powtongsook, P. Pavasant, Enhanced productivity of *Chaetoceros calcitrans* in airlift photobioreactors, Bioresour. Technol. 98 (2007) 2123–2130.

[19] E. Granum, S.M. Myklestad, A photobioreactor with pH control: demonstration by growth of the marine diatom *Skeletonema costatum*, J. Plankton Res. 24 (2002) 557–563.

[20] F.A. Fernández, J.S. Perez, J.F. Sevilla, F.G. Camacho, E.M. Grima, Modeling of eicosapentaenoic acid (EPA) production from *Phaeodactylum tricornutum* cultures in tubular photobioreactors. Effects of dilution rate, tube diameter, and solar irradiance, Biotechnol. Bioeng. 68 (2000) 173–183.

[21] T. Li, M. Strous, M. Melkonian, Biofilm-based photobioreactors: their design and improving productivity through efficient supply of dissolved inorganic carbon, FEMS Microbiol. Lett. 364 (2017).

[22] M. Gross, W. Henry, C. Michael, Z. Wen, Development of a rotating algal biofilm growth system for attached microalgae growth with in situ biomass harvest, Bioresour. Technol. 150 (2013) 195–201.

[23] M.B. Johnson, Z. Wen, Development of an attached microalgal growth system for biofuel production, Appl. Microbiol. Biotechnol. 85 (2010) 525–534.

[24] E. Cointet, E. Séverin, A. Couzinet-Mossion, V. Méléder, O. Gonçalves, G. Wielgosz-Collin, Assessment of the lipid production potential of six benthic diatom species grown in airlift

photobioreactors, J. Appl. Phycol. (2021) 1–11.

[25] E.C. Nowack, B. Podola, M. Melkonian, The 96-well twin-layer system: a novel approach in the cultivation of microalgae, Protist. 156 (2005) 239–251.

[26] J. Shi, B. Podola, M. Melkonian, Removal of nitrogen and phosphorus from wastewater using microalgae immobilized on twin layers: an experimental study, J. Appl. Phycol. 19 (2007) 417–423.

[27] F. Gao, Z.-H. Yang, C. Li, G.-M. Zeng, D.-H. Ma, L. Zhou, A novel algal biofilm membrane photobioreactor for attached microalgae growth and nutrients removal from secondary effluent, Bioresour. Technol. 179 (2015) 8–12.

[28] T. Naumann, Z. Çebi, B. Podola, M. Melkonian, Growing microalgae as aquaculture feeds on twin-layers: a novel solid-state photobioreactor, J. Appl. Phycol. 25 (2013) 1413–1420.

[29] F. Berner, K. Heimann, M. Sheehan, Microalgal biofilms for biomass production, J. Appl. Phycol. 27 (2015) 1793–1804.

[30] R.M. Benstein, Z. Çebi, B. Podola, M. Melkonian, Immobilized growth of the peridinin-producing marine dinoflagellate *Symbiodinium* in a simple biofilm photobioreactor, Mar. Biotechnol. 16 (2014) 621–628.

[31] R.R. Guillard, Culture of phytoplankton for feeding marine invertebrates, in: Cult. Mar. Invertebr. Anim., Springer, 1975: pp. 29–60.

[32] C. Büchel, C. Wilhelm, In vivo analysis of slow chlorophyll fluorescence induction kinetics in algae: progress, problems and perspectives, Photochem. Photobiol. 58 (1993) 137–148.

[33] J. Rijstenbil, Effects of UVB radiation and salt stress on growth, pigments and antioxidative defence of the marine diatom *Cylindrotheca closterium*, Mar. Ecol. Prog. Ser. 254 (2003) 37–48.

[34] A. Michelle Wood, R. Everroad, L. Wingard, Measuring growth rates in microalgal cultures, in: R.A. Andersen (Ed.), Algal Cult. Tech., Elsevier, 2005: p. 269.

[35] E.G. Bligh, W.J. Dyer, A rapid method of total lipid extraction and purification, Can. J. Biochem. Physiol. 37 (1959) 911–917.

[36] A. Aminot, R. Kérouel, Dosage automatique des nutriments dans les eaux marines: méthodes en flux continu, Editions Quae, 2007.

[37] V. Méléder, Y. Rincé, L. Barillé, P. Gaudin, P. Rosa, Spatiotemporal changes in microphytobenthos assemblages in a macrotidal flat (Bourgneuf Bay, France) 1, J. Phycol. 43 (2007) 1177–1190.

[38] E. Cointet, Diatomées marines benthiques : une ressource originale de souches “oléagineuses” pour une application en santé et nutrition [dissertation], Université de Nantes, 2019.

[39] V. Méléder, L. Barillé, P. Launeau, V. Carrère, Y. Rincé, Spectrometric constraint in analysis of benthic diatom biomass using monospecific cultures, Remote Sens. Environ. 88 (2003) 386–400.

[40] L. Barillé, J.-L. Mouget, V. Méléder, P. Rosa, B. Jesus, Spectral response of benthic diatoms with different sediment backgrounds, Remote Sens. Environ. 115 (2011) 1034–1042.

[41] S. Sma-Air, R.J. Ritchie, Spectrofluorometric Insights into the Application of PAM Fluorometry in Photosynthetic Research, Photochem. Photobiol. 97 (2021) 991–1000.

[42] M. Consalvey, R.G. Perkins, D.M. Paterson, G.J. Underwood, PAM fluorescence: a beginners guide for benthic diatomists, Diatom Res. 20 (2005) 1–22.

[43] K.A. Gomez, A.A. Gomez, Statistical procedures for agricultural research, John Wiley & sons, 1984.

[44] M.R. de la Peña, Cell growth and nutritive value of the tropical benthic diatom, *Amphora* sp., at varying levels of nutrients and light intensity, and different culture locations, J. Appl. Phycol. 19 (2007) 647–655.

[45] I. Indrayani, N.R. Mohamani, M.A. Borowitzka, Long-term reliable culture of a halophilic diatom, *Amphora* sp. MUR258, in outdoor raceway ponds, J. Appl. Phycol. 31 (2019) 2771–2778.

[46] A. Richmond, Outdoor mass cultures of microalgae, in: Handb. Microalgal Mass Cult., CRC Press, 1986: pp. 285–330.

[47] J. Masojídek, C. Gómez-Serrano, K. Ranglová, B. Cicchi, Á. Encinas Bogeat, J.A. Câmara Manoel, A. Sanches Zurano, A.M. Silva Benavides, M. Barceló-Villalobos, V.A. Robles Carnero, Photosynthesis monitoring in microalgae cultures grown on municipal wastewater as a nutrient source in large-scale outdoor bioreactors, Biology. 11 (2022) 1380.

[48] E. Posadas, S. Bochon, M. Coca, M. García-González, P. García-Encina, R. Muñoz, Microalgae-based agro-industrial wastewater treatment: a preliminary screening of biodegradability, J. Appl.

Phycol. 26 (2014) 2335–2345.

[49] S.-H. Lee, H.-M. Oh, B.-H. Jo, S.-A. Lee, S.-Y. Shin, H.-S. Kim, S.-H. Lee, C.-Y. Ahn, Higher biomass productivity of microalgae in an attached growth system, using wastewater, J. Microbiol. Biotechnol. 24 (2014) 1566–1573.

[50] L.-L. Zhuang, D. Yu, J. Zhang, F. Liu, Y.-H. Wu, T.-Y. Zhang, G.-H. Dao, H.-Y. Hu, The characteristics and influencing factors of the attached microalgae cultivation: A review, Renew. Sustain. Energy Rev. 94 (2018) 1110–1119.

[51] A. Ozkan, H. Berberoglu, Cell to substratum and cell to cell interactions of microalgae, Colloids Surf. B Biointerfaces. 112 (2013) 302–309.

[52] L.B. Christenson, R.C. Sims, Rotating algal biofilm reactor and spool harvester for wastewater treatment with biofuels by-products, Biotechnol. Bioeng. 109 (2012) 1674–1684.

[53] L. Stal, J. De Brouwer, Biofilm formation by benthic diatoms and their influence on the stabilization of intertidal mudflats, Berichte-Forschungszentrum Terramare. 12 (2003) 109–111.

[54] M. Consalvey, D.M. Paterson, G.J. Underwood, The ups and downs of life in a benthic biofilm: migration of benthic diatoms, Diatom Res. 19 (2004) 181–202.

[55] S.N. Genin, J.S. Aitchison, D.G. Allen, Design of algal film photobioreactors: material surface energy effects on algal film productivity, colonization and lipid content, Bioresour. Technol. 155 (2014) 136–143.

[56] N. Boelee, M. Janssen, H. Temmink, R. Shrestha, C. Buisman, R. Wijffels, Nutrient removal and biomass production in an outdoor pilot-scale phototrophic biofilm reactor for effluent polishing, Appl. Biochem. Biotechnol. 172 (2014) 405–422.

[57] L.B. Christenson, R.C. Sims, Rotating algal biofilm reactor and spool harvester for wastewater treatment with biofuels by-products, Biotechnol. Bioeng. 109 (2012) 1674–1684.

[58] T.E. Murphy, H. Berberoglu, Flux balancing of light and nutrients in a biofilm photobioreactor for maximizing photosynthetic productivity, Biotechnol. Prog. 30 (2014) 348–359.

[59] T. Li, B. Piltz, B. Podola, A. Dron, D. de Beer, M. Melkonian, Microscale profiling of photosynthesis-related variables in a highly productive biofilm photobioreactor, Biotechnol. Bioeng. 113 (2016) 1046–1055.

[60] G. Wolf, C. Picioreanu, M.C. van Loosdrecht, Kinetic modeling of phototrophic biofilms: the PHOBIA model, Biotechnol. Bioeng. 97 (2007) 1064–1079.

[61] A. Wulff, K. Zacher, D. Hanelt, A. Al-Handal, C. Wiencke, UV radiation-a threat to Antarctic benthic marine diatoms?, Antarct. Sci. 20 (2008) 13–20.

[62] Y. Huang, P. Li, Y. Huang, A. Xia, X. Zhu, Q. Liao, A synchronous photoautotrophic-heterotrophic biofilm cultivation mode for *Chlorella vulgaris* biomass and lipid simultaneous accumulation, J. Clean. Prod. 336 (2022) 130453.

[63] E. Cointet, G. Wielgosz-Collin, G. Bougaran, V. Rabesaotra, C. Goncalves, V. Meleder, Effects of light and nitrogen availability on photosynthetic efficiency and fatty acid content of three original benthic diatom strains, PLoS One. 14 (2019).

[64] R.J. Geider, J. La Roche, R.M. Greene, M. Olaizola, Response of the photosynthetic apparatus of *Phaeodactylum tricornutum* (Bacillariophyceae) to nitrate, phosphate, or iron starvation, J. Phycol. 29 (1993) 755–766.

[65] S. Lippemeier, P. Hartig, F. Colijn, Direct impact of silicate on the photosynthetic performance of the diatom *Thalassiosira weissflogii* assessed by on-and off-line PAM fluorescence measurements., J. Plankton Res. 21 (1999).

[66] E.B. Young, J. Beardall, Photosynthetic function in *Dunaliella tertiolecta* (Chlorophyta) during a nitrogen starvation and recovery cycle, J. Phycol. 39 (2003) 897–905.

[67] M.A. Brzezinski, The Si: C: N ratio of marine diatoms: interspecific variability and the effect of some environmental variables, J. Phycol. 21 (1985) 347–357.

[68] R.N. Xuan, J. Mouget, V. Turpin, P. Jaouen, J. Pruvost, Optimization of the growth and marennine production by the diatom *Haslea ostrearia* in photobioreactor, Algal Res. 55 (2021) 102251.

[69] P. Heraud, J. Beardall, Changes in chlorophyll fluorescence during exposure of *Dunaliella tertiolecta* to UV radiation indicate a dynamic interaction between damage and repair processes, Photosynth. Res. 63 (2000) 123–134.

Author contributions

M.D.G.A. as Ph.D. student was involved at all study stages including biomass production and sample preparation, and data presentation and interpretation, and initial write-up. N.D.G. and A.J. as training students helped M.D.G.A. to obtain samples using Fernbach and realized particularly lipid analyses. R.V. contributed to lipid extractions, lipid class separations and chemical derivatizations, and performed the GC/MS analyses. A.M., G.W.C. and V.M. initiated and supervised the Ph.D. thesis work of M.D.G.A. and were responsible for writing, arranging and checking the manuscript. All authors read and approved the final manuscript.

Declaration of interests

☒The authors declare that they have no known competing financial interests or personal relationships that could have appeared to influence the work reported in this paper.

☐The authors declare the following financial interests/personal relationships which may be considered as potential competing interests:

Highlights

- A commercial suspension PBR was adapted to build a vertical tubular lab-scale PSBR
- Marine benthic diatom *Amphora* sp. NCC169 was cultivated in Fernbach flasks and PSBR
- Diatom biomass and lipid yield in PSBR are higher than in Fernbach flasks